



The role of apparent diffusion coefficient value in the diagnosis of localized type 1 autoimmune pancreatitis: differentiation from pancreatic ductal adenocarcinoma and evaluation of response to steroids

Tsuyoshi Sekito¹ · Yasutaka Ishii¹ · Masahiro Serikawa¹ · Tomofumi Tsuboi¹ · Ryota Kawamura¹ · Ken Tsushima¹ · Shinya Nakamura¹ · Tetsuro Hirano¹ · Ayami Fukiage¹ · Takeshi Mori¹ · Juri Ikemoto¹ · Yusuke Kiyoshita¹ · Sho Saeki¹ · Yosuke Tamura¹ · Sayaka Miyamoto¹ · Kazuaki Chayama^{1,2,3}

Received: 9 October 2020 / Revised: 5 December 2020 / Accepted: 7 December 2020 / Published online: 1 January 2021
© The Author(s), under exclusive licence to Springer Science+Business Media, LLC part of Springer Nature 2021

Abstract

Purpose The aim of this study was to clarify the usefulness of the apparent diffusion coefficient (ADC) value in the differential diagnosis of localized autoimmune pancreatitis (AIP) and pancreatic ductal adenocarcinoma (PDAC) and the evaluation of response to steroids.

Methods This study retrospectively analyzed 40 patients with localized AIP and 71 patients with PDAC who underwent abdominal MRI with DWI ($b=0$ and 1000 s/mm²). Their ADC values at the lesion sites and five MRI findings useful for diagnosing AIP were evaluated. In addition, ADC values before and after steroid therapy were compared in 28 patients with localized AIP.

Results The median ADC value was significantly lower for localized AIP than for PDAC (1.057×10^{-3} vs 1.376×10^{-3} mm²/s, $P < 0.001$). In the ROC curve analysis, the area under the curve was 0.957 and optimal cut-off value of ADC for differentiating localized AIP from PDAC was 1.188×10^{-3} mm²/s. ADC value $\leq 1.188 \times 10^{-3}$ mm²/s showed the highest sensitivity and accuracy among the MRI findings (92.6% and 90.7%, respectively), and when combined with one or more other MRI findings, showed 96.3% specificity. The median ADC values before and after steroid therapy (mean 7.9 days) were 1.061×10^{-3} and 1.340×10^{-3} mm²/s, respectively, and ADC values were significantly elevated after steroid induction ($P < 0.001$).

Conclusion The measurement of ADC values was useful for the differential diagnosis of localized AIP and PDAC and for the early determination of the effect of steroid therapy.

Keywords Autoimmune pancreatitis · Apparent diffusion coefficient · Diffusion-weighted imaging · Pancreatic ductal adenocarcinoma · Steroid therapy

Introduction

Autoimmune pancreatitis (AIP) is a distinct form of pancreatitis characterized clinically by frequent presentation with obstructive jaundice with or without a pancreatic mass, histologically by a lymphoplasmacytic infiltrate and fibrosis and therapeutically by a dramatic response to steroids [1]. AIP is classified as two subtypes, type 1 and type 2. Type 1 AIP is a pancreatic manifestation of an IgG4-related disease and most of AIP are type 1 AIP in Asia. On the other hand, type 2 AIP, which is commonly observed in Europe and the United States and extremely rare in Asia, shows idiopathic duct-centric pancreatitis

✉ Yasutaka Ishii
yishii@hiroshima-u.ac.jp

¹ Department of Gastroenterology and Metabolism, Graduate School of Biomedical & Health Sciences, Hiroshima University, 1-2-3 Kasumi, Minami-ku, Hiroshima 734-8551, Japan

² Research Center for Hepatology and Gastroenterology, Hiroshima University, Hiroshima, Japan

³ RIKEN Center for Integrative Medical Sciences, Yokohama, Japan

characterized by granulocytic epithelial lesion [2] and is a different condition from type 1 AIP. Based on the International Consensus Diagnostic Criteria (ICDC) [1] and Japanese diagnostic criteria [3], type 1 AIP is comprehensively diagnosed based on pancreatic imaging findings, serum IgG4 level, extra-pancreatic lesions, histopathological findings, and steroid responsiveness. Diagnosis of typical type 1 AIP cases with diffuse pancreatic enlargement with capsule-like rim [4] on computed tomography (CT) or magnetic resonance imaging (MRI) is relatively easy, but AIP cases with atypical pancreatic parenchymal findings, such as localized enlargement or mass formation, are difficult not only to diagnose as AIP but also to differentiate from pancreatic ductal adenocarcinoma (PDAC). According to the ICDC diagnostic algorithm for type 1 AIP, patients with atypical pancreatic parenchymal findings on CT or MRI should be managed as PDAC [1]. Endoscopic ultrasound-guided fine needle aspiration (EUS-FNA) has high sensitivity and specificity for diagnosing PDAC [5, 6], and it is a very useful examination for differentiating AIP from PDAC. However, approximately 10% of PDAC are false-negative with EUS-FNA, and the results of histopathological diagnoses of AIP by EUS-FNA vary widely [7–10], making diagnosis difficult in some cases. In addition, when diagnosing patients suspected of type 1 AIP with atypical pancreatic parenchymal findings, it is often necessary to evaluate steroid responsiveness after excluding PDAC by using examinations including EUS-FNA. Although it is recommended that steroid responsiveness be assessed in about 2 weeks [1, 11], there have been few reports on the duration of steroid trials and there is insufficient evidence on imaging methods used to evaluate efficacy.

MRI is the first imaging procedure performed in the diagnosis of AIP along with CT [1]. MRI provides better tissue contrast and the pancreatic duct can be evaluated by magnetic resonance cholangiopancreatography (MRCP) [12, 13]. In fact, it has been reported that MRI has a better diagnostic performance than CT in differentiating non-diffuse-type AIP from PDAC [14]. Diffusion-weighted imaging (DWI), which is one of the sequences of MRI, exploits the random motion of water molecules [15], and its usefulness in the diagnosis of PDAC has been reported [16, 17]. Quantitative analysis can be performed with the generation of apparent diffusion coefficient (ADC) maps from diffusion images obtained at different b values [18], and calculated values are called ADC values. The usefulness of ADC values has been reported in differentiating AIP from PDAC [19–22]. In addition, some reports have examined changes in ADC values before and after steroid induction [19, 23, 24]. However, all previous studies evaluating the ADC value of localized AIP have targeted a small number of AIP patients, specifically 4 to 15 patients with an average of 11, and the changes in ADC values

about 2 weeks after the induction of steroid, which is recommended in the guidelines [1, 11] as the timing of efficacy evaluation, are unclear.

This study aimed to confirm the usefulness of ADC value measurement in the differential diagnosis from PDAC and the early evaluation of the effect of steroid therapy in a larger number of patients with localized type 1 AIP.

Materials and methods

Patients

This study retrospectively analyzed a total of 40 consecutive patients with localized type 1 AIP who underwent abdominal MRI from April 2010 to March 2020 at our institution at the time of initial diagnosis or pancreatic relapse. AIP was diagnosed based on ICDC [1]. The localized type included both segmental type and focal type [1, 3], and the range of each enlargement was defined as 1/3 to 2/3 of the whole pancreas and less than 1/3 of the whole pancreas. Thirty-three patients (82.5%) received steroid therapy. Based on the Japanese consensus guidelines [25], steroid therapy was indicated for patients with symptoms such as obstructive jaundice, abdominal pain, back pain, and extra-pancreatic lesions, but in 13 patients (32.5%), steroid therapy also had a diagnostic trial implication. In principle, the initial dose of oral prednisolone was 30–40 mg/day (approximately 0.6 mg/kg/day) as recommended in the guideline [25]. Four patients underwent surgical resection because the pancreatic neoplasm could not be completely ruled out.

This study also included 71 patients histopathologically diagnosed with PDAC who underwent an abdominal MRI with DWI during the same period. Contrast-enhanced CT was routinely performed at our institution for staging PDAC. MRI was performed in the patients in which contrast-enhanced CT could not be performed due to iodine contrast agent allergy or reduced renal function, liver metastasis was suspected by CT or ultrasonography, or it was difficult to distinguish from mass-forming pancreatitis including AIP. Definitive histopathological diagnosis was made by surgical resection in 43 patients and by EUS-FNA in 28 patients due to unresectability. In patients undergoing neoadjuvant chemotherapy, ADC values were measured by MRI before starting chemotherapy.

This study was conducted in accordance with the Declaration of Helsinki and was approved by the Ethical Committee for Epidemiology of our institution (approval no. E-1949). The written informed consent was waived by the Institutional Review Board because this was a retrospective study of clinical and image data.

MRI techniques

MRI examinations were conducted from April 2010 to September 2014 with a 1.5 T superconducting scanner (SIGNA Excite HD, GE Healthcare, Milwaukee, WI, USA) and from October 2014 with a 3 T superconducting scanner (Vantage Titan, Toshiba Medical Systems, Tochigi, Japan). Our MRI protocol for the pancreas included T1-weighted imaging (T1WI), T2-weighted imaging (T2WI), three-dimensional (3D) MRCP, and DWI (Table 1). T1WI was performed using in-phase and out-of-phase spoiled gradient echo (GRE) sequence, and the technical parameters of each MRI scanners were as follows: repetition time (TR), 200 ms, and 170 ms; in-phase echo time (TE), 4.2 ms and 2.3 ms; out-of-phase TE, 2.1 ms and 1.15 ms; flip angle (FA), 80° and 60°; image matrix, 256 × 192 and 288 × 192; field of view (FOV), both at 360 mm; slice thickness, both at 6 mm. T2WI was performed using respiratory-triggered fast spin-echo (FSE) sequence and breath-hold FSE sequence with the following parameters, respectively: TR, 4350 ms and 3400 ms; TE, both at 90 ms; FA, 90–180° and 90–120°; image matrix, 320 × 192 and 336 × 192; FOV, both at 360 mm; slice thickness, both at 6 mm. 3D-MRCP was performed using respiratory-triggered FSE sequence and fast advanced spin-echo sequence with the following parameters, respectively: TR, 3750 ms and 6000 ms; TE, 500 ms and 390 ms; FA, 90–180° and 90–120°; image matrix, 256 × 224 and 448 × 224; FOV, both at 320 mm; slice thickness, both at 2 mm. DWI was performed using single-shot spin-echo (SSSE) sequence under free breathing and respiratory-triggered SSSE echo planar imaging with the following parameters, respectively: TR, 6000 ms and 3000–5000 ms; TE, 74 ms and 64 ms; FA, both at 90°; image matrix, 128 × 192 and 128 × 144; FOV, both at 360 mm; image direction, both axial; slice thickness/slice gap, both at 6/1 mm; number of acquisition, 6 and 3;

b value, both at 1000 s/mm²; directions of motion probing gradient, both at three directions (phase, read out, and slice).

Dynamic contrast-enhanced MRI using gadopentetate dimeglumine (Magnevist, Bayer AG, Leverkusen, Germany) or gadobutrol (Gadovist, Bayer AG) was performed in 27 patients (67.5%) with localized AIP and 27 patients (38.0%) with PDAC. Precontrast fat-saturated T1WI was performed using 3D spoiled GRE (liver acquisition with volume acceleration, LAVA) and 3D Fast GRE with the following parameters, respectively: TR, 3.8 ms and 3.7 ms; TE, 1.9 ms and 1.3 ms; FA, 12° and 15°; image matrix, 320 × 192 and 256 × 224; FOV, both at 360 mm; slice thickness, 5 mm and 4 mm. The pancreatic phase (45 s), portal phase (90 s), and delayed phase (3 min) were obtained after intravenous injection of the contrast agent at a rate of 1 ml/s using a power injector, followed by a 20 ml of saline.

Image analysis

All MRI images were reviewed by two gastroenterologists with over 15 years of experience in evaluating images of pancreas disease. (Y.I. and M.S.). Both reviewers were blinded to the clinical diagnosis. ADC maps were created by the application of each system. A circular region of interest (ROI) was drawn on the lesion in the ADC map, and the ADC value was measured three times to calculate the mean value. ROIs were drawn avoiding the periphery of the lesion and in PDAC avoiding the necrotic and cystic areas. The mean ROI size was 93 ± 48 [SD] mm². ADC values were calculated using the two-point method with the formula $ADC = \ln(S1/S2)/(b2 - b1)$. Note that ln is a natural logarithm and S1 and S2 are signal intensities of the lesion obtained using DWI at *b*₁ (0 s/mm²) and *b*₂ (1000 s/mm²), respectively. In 28 AIP patients, MRI was performed before

Table 1 MRI protocols

Parameters	T1WI		T2WI		3D-MRCP		DWI	
	1.5 T scanner	3 T scanner	1.5 T scanner	3 T scanner	1.5 T scanner	3 T scanner	1.5 T scanner	3 T scanner
Sequence type	Spoiled GRE	Spoiled GRE	RT-FSE	BH-FSE	RT-FSE	FASE	SSSE	RT-SSSE EPI
TR (ms)	200	170	4350	3400	3750	6000	6000	3000–5000
TE (ms)	4.2–2.1	2.3–1.15	90	90	500	390	74	64
FA (°)	80	60	90–180	90–120	90–180	90–120	90	90
Image matrix	256 × 192	288 × 192	320 × 192	336 × 192	256 × 224	448 × 224	128 × 192	128 × 144
FOV (mm)	360	360	360	360	320	320	360	360
slice thickness (mm)	6	6	6	6	2	2	6	6
No. of acquisition	1	1	1	1	1	1	6	3

1.5 T scanner = SIGNA Excite HD, GE Healthcare; 3 T scanner = Vantage Titan, Toshiba Medical Systems; T1WI, T1-weighted imaging; T2WI, T2-weighted imaging; 3D-MRCP, three-dimensional magnetic resonance cholangiopancreatography; DWI, diffusion weighted imaging; GRE, gradient echo; RT, respiratory-triggered; FSE, fast spin-echo; BH, breath-hold; FASE, fast advanced spin echo; SSSE, single-shot spin-echo; EPI, echo planar imaging; TR, repetition time; TE, echo time; FA, flip angle; FOV, field of view

and about 1 week after the induction of steroid therapy, and ADC values were measured.

In addition, the following MRI findings, which have been reported to be useful in distinguishing localized AIP from PDAC, were evaluated [14, 20–22, 26–29]: (1) hypointense capsule-like rim on T2WI; (2) speckled/dotted enhancement on the pancreatic phase; (3) delayed homogeneous enhancement; (4) duct penetrating sign; and (5) main pancreatic duct (MPD) upstream dilatation ≤ 4 mm. The duct penetrating sign and MPD diameter were evaluated by MRCP.

Statistical analysis

Statistical analyses were performed using JMP Pro 14.2.0 (SAS Institute Inc. Cary, NC, USA). The Wilcoxon rank sum test was used to compare ADC values between localized AIP and PDAC, and between MRI scanners. The Wilcoxon signed rank test was used to compare ADC values before and after steroid therapy. Receiver operator characteristic (ROC) analysis was performed to evaluate the diagnostic ability of ADC values in differentiating localized AIP from PDAC. The Chi square test or Fisher's exact test was used for the comparison of MRI findings between localized AIP and PDAC. *P* values < 0.05 were considered statistically significant.

Results

Patient characteristics

The clinical profiles of all 40 patients with localized type 1 AIP are shown in Table 2. The median age was 67 years (interquartile range [IQR] 58–73 years), and there were 37 men and 3 women. The extent of pancreatic enlargement was segmental in 12 patients (pancreatic head–body in 6 patients and pancreatic body–tail in 6 patients) and focal in 28 patients (pancreatic head in 17 patients, pancreatic body in 4 patients, and pancreatic tail in 7 patients). The median lesion diameter was 31 mm (IQR 26–50 mm). The median serum IgG4 level was 281 mg/dl (IQR 162–399 mg/dl), and 35 patients (87.5%) showed an elevated serum IgG4 level (≥ 135 mg/dl). Extra-pancreatic lesions were observed in 15 patients (37.5%), including 3 patients with extra-pancreatic sclerosing cholangitis, 6 patients with retroperitoneal fibrosis, 6 patients with sclerosing dacryoadenitis/sialadenitis, and 2 patients with kidney lesion. EUS-FNA was performed in 38 patients (95.0%), and eight patients met ICDC level 2 and none met level 1. No patients were diagnosed of malignant disease by EUS-FNA. The final diagnosis based on ICDC¹ was definitive in 33 patients and probable in seven patients. MRI was performed at the time of initial diagnosis in 32 patients and pancreatic relapse in eight patients.

Table 2 Clinical profiles of the 40 patients with localized type 1 AIP

Characteristics	Values
Age (years)	67 (58–73)
Sex (male to female)	37:3
Enlargement of the pancreas, <i>n</i> (%)	
Segmental	12 (30.0%)
Head–body	6 (15.0%)
Body–tail	6 (15.0%)
Focal	28 (70.0%)
Head	17 (42.5%)
Body	4 (10.0%)
Tail	7 (17.5%)
Lesion diameter (mm)	31 (26–50)
Serological findings	
Serum IgG4 (mg/dL)	281 (162–399)
Elevated serum IgG4 level (≥ 135 mg/dL), <i>n</i> (%)	35 (87.5%)
Other organ involvement, <i>n</i> (%)	14 (35.0%)
Extra-pancreatic sclerosing cholangitis	3 (7.5%)
Sclerosing dacryoadenitis/sialadenitis	6 (15.0%)
Retroperitoneal fibrosis	6 (15.0%)
Kidney lesion	2 (5.0%)
Diagnosis, <i>n</i> (%)	
Definitive	33 (82.5%)
Probable	7 (17.5%)
Steroid therapy, <i>n</i> (%)	33 (82.5%)

Data are expressed as number (percentage) or median (interquartile range)

AIP autoimmune pancreatitis

On the contrary, for PDAC patients, the median age was 68 years (IQR 58–76 years), and there were 43 men and 28 women. The tumors were located in the pancreatic head in 40 patients, pancreatic body in 19 patients, and pancreatic tail in 12 patients, with a median tumor diameter of 28 mm (IQR 20–40 mm).

Comparison of ADC values between localized AIP and PDAC

On DWI, the lesion site showed hyperintense signal in 39 patients (97.5%) with localized AIP (Fig. 1) and 71 patients (100%) with PDAC (Fig. 2). The median ADC value of localized AIP was 1.057×10^{-3} mm²/s (IQR, 0.996 – 1.142×10^{-3} mm²/s), and there was no difference in ADC values based on the extent of pancreatic enlargement (segmental; 1.038×10^{-3} mm²/s, focal; 1.072×10^{-3} mm²/s, *P* = 0.871). No associations were found between ADC values and other clinical parameters (age, sex, serum IgG4 level, and presence or absence of extra-pancreatic lesions). On the contrary, the median ADC value of PDAC was 1.376×10^{-3} mm²/s (IQR 1.267 – 1.523×10^{-3} mm²/s),

Fig. 1 A 44-year-old man with localized type 1 autoimmune pancreatitis. **a** T2-weighted image shows the mass in the pancreatic tail (arrow). **b** Diffusion-weighted imaging at $b = 1000 \text{ s/mm}^2$. The mass shows hyperintense signal (arrow). **c** ADC map of the same lesion. The mass shows hypointense signal (arrow). **d** Measurement of ADC values. The regions of interest were set within the lesion. The measured ADC values were displayed in a white flame below the image ($0.832, 0.858, \text{ and } 0.897 \times 10^{-3} \text{ mm}^2/\text{s}$). *ADC* apparent diffusion coefficient

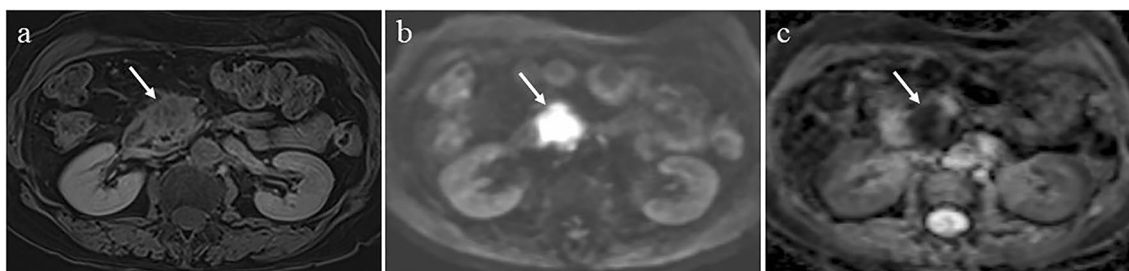
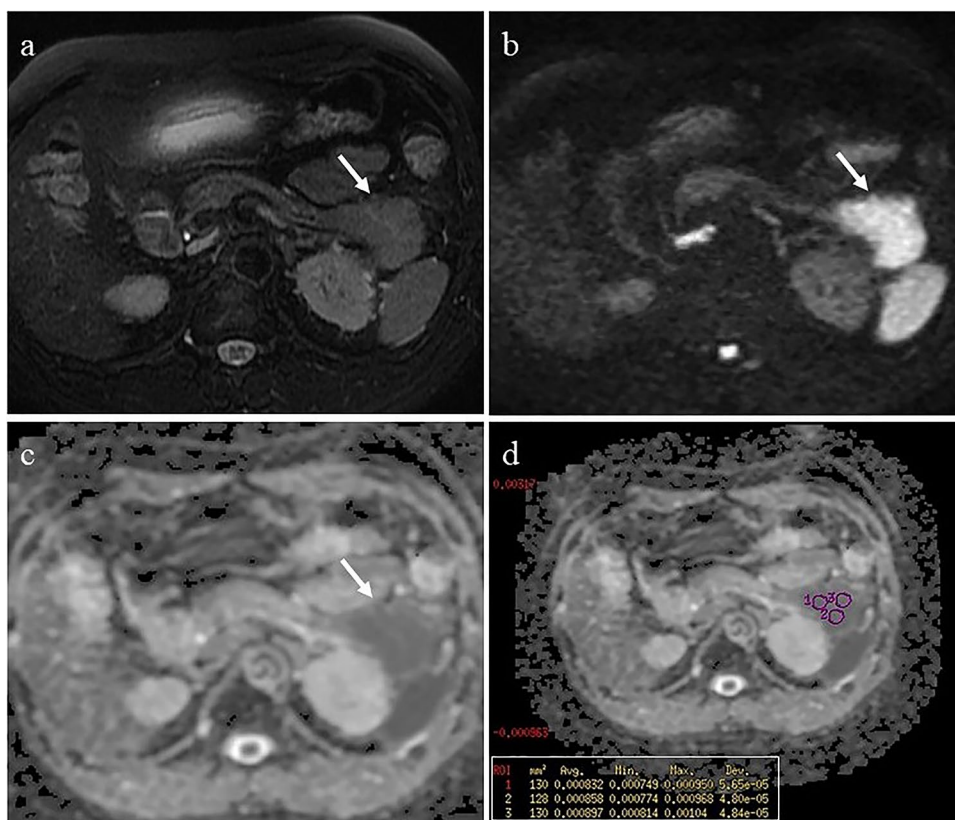


Fig. 2 A 63-year-old woman with pancreatic ductal adenocarcinoma. **a** Delayed-phase magnetic resonance image shows the pancreatic head mass heterogeneously enhanced (arrow). **b** Diffusion-weighted imaging at $b = 1000 \text{ s/mm}^2$. The mass in the pancreatic head shows

hyperintense signal (arrow). **c** ADC map of the same lesion. The mass shows hypointense signal (arrow). The ADC value of the mass was $1.525 \times 10^{-3} \text{ mm}^2/\text{s}$. *ADC* apparent diffusion coefficient

which was significantly higher than the ADC value of localized AIP (Fig. 3, $P < 0.001$). The ROC analysis showed that the area under the ROC curve (AUC) was 0.957 (Fig. 4). When the cut-off value was $1.188 \times 10^{-3} \text{ mm}^2/\text{s}$, the diagnosis of localized AIP was 95.0% for sensitivity and 90.1% for specificity.

The 1.5 T MRI was used on 18 localized AIP patients and 23 PDAC patients, and the 3 T MRI was used on 22 localized AIP patients and 48 PDAC patients. No significant differences were found in the ADC values between the MRI scanners for either localized AIP or PDAC ($P = 0.654$ and 0.778 , respectively) (Table 3).

Diagnostic performance of MRI findings

A comparison of MRI findings between localized AIP and PDAC is shown in Table 4. All five MRI findings were observed significantly more frequently in patients with localized AIP than patients with PDAC (all $P < 0.001$).

The diagnostic performance of MRI findings in the diagnosis of localized AIP was evaluated in 54 patients (27 localized AIP and 27 PDAC) who underwent gadolinium-enhanced MRI so that all six MRI findings, including the ADC value $\leq 1.188 \times 10^{-3} \text{ mm}^2/\text{s}$, could be evaluated in each patient (Table 5). The ADC value $\leq 1.188 \times 10^{-3}$

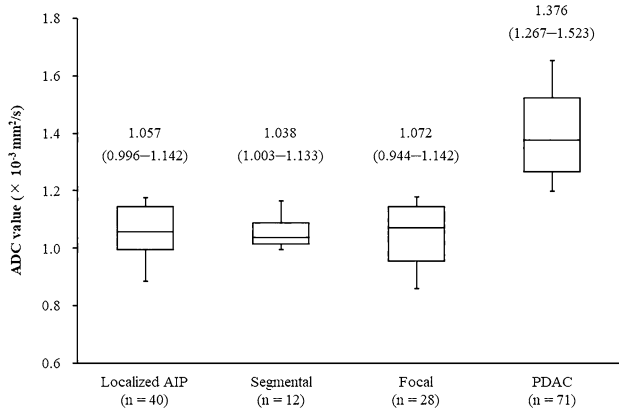


Fig. 3 Box-and-whisker plots of the ADC values of localized AIP, segmental type AIP, focal type AIP, and PDAC. Median ADC value of localized AIP was significantly lower than that of PDAC ($P < 0.001$). *ADC* apparent diffusion coefficient, *AIP* autoimmune pancreatitis, *PDAC* pancreatic ductal adenocarcinoma

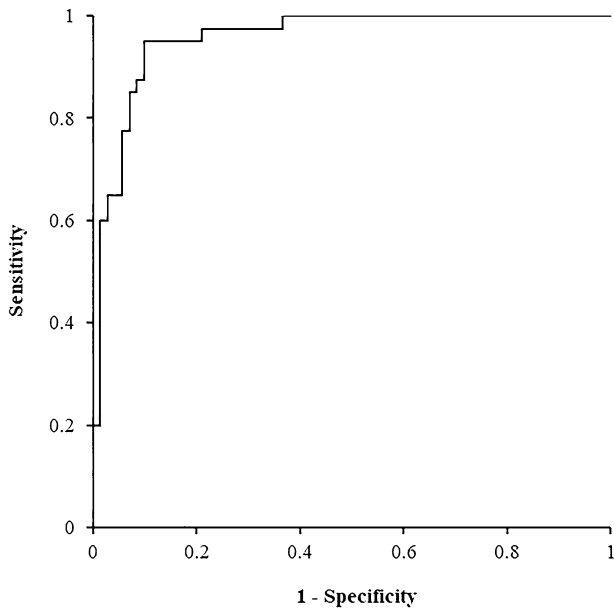


Fig. 4 ROC curve of ADC values for differentiation between localized AIP and PDAC. The area under the ROC curve was 0.957, and the sensitivity and specificity were 95.0% and 90.1%, respectively, when the cut-off value was set to $1.188 \times 10^{-3} \text{ mm}^2/\text{s}$. *ROC* receiver operating characteristic, *ADC* apparent diffusion coefficient, *AIP* autoimmune pancreatitis, *PDAC* pancreatic ductal adenocarcinoma

mm^2/s had the highest sensitivity, accuracy, and odds ratio (92.6%, 90.7%, and 100.0, respectively). On the other hand, the specificity was highest at 100% in the hypointense capsule-like rim, but the sensitivity was only 37.0%. Regarding the combination of MRI findings, when any one or more the other five findings were combined with the ADC value $\leq 1.188 \times 10^{-3} \text{ mm}^2/\text{s}$, sensitivity, specificity, and accuracy of 92% or more and the odds ratio of 325.0 (95% confidence intervals, 27.7–3813.2) were obtained. These values were much higher than when any two or more MRI findings excluding the ADC value were combined.

Changes in ADC value by steroid induction in localized AIP

ADC values at lesion site were measured before and after steroid therapy in 28 localized AIP patients (median age, 66 years; sex, 25 men and 3 women; extent of pancreatic enlargement, segmental 10 patients and focal 18 patients) (Fig. 5). MRI was performed on mean 7.9 ± 1.7 [SD] days after steroid induction. The median ADC values before and after steroid induction were $1.061 \times 10^{-3} \text{ mm}^2/\text{s}$ (IQR $0.974\text{--}1.144 \times 10^{-3} \text{ mm}^2/\text{s}$) and $1.340 \times 10^{-3} \text{ mm}^2/\text{s}$ (IQR $1.234\text{--}1.454 \times 10^{-3} \text{ mm}^2/\text{s}$), respectively, and a significant increase in ADC values was observed (Fig. 6, $P < 0.001$). The median rate of change in ADC value was 22.0% (IQR 17.3–27.1%), and there were no patients in which ADC value decreased after steroid induction. One patient showed little change in ADC value (change rate $< 1\%$) and no improvement in pancreatic enlargement, but this patient had been prescribed azathioprine for ulcerative colitis and his oral prednisolone dose had been reduced to only half the normal dose.

Discussion

Typical cases with type 1 AIP present with diffuse pancreatic enlargement with delayed enhancement on contrast-enhanced CT or MRI, but approximately 45% of cases are atypical with localized pancreatic enlargement [30]. In the diagnosis of localized AIP, differentiation from pancreatic tumors, especially PDAC, is extremely important but remains a clinical challenge. Kamisawa et al. [31] reported

Table 3 Comparison of ADC values between MRI scanners

Diagnosis	GE SIGNA™ Excite HD 1.5T (n = 41)	Toshiba Vantage Titan™ 3T (n = 70)	P value
Localized AIP (n = 40)	1.052 (0.924–1.140) $\times 10^{-3} \text{ mm}^2/\text{s}$	1.065 (0.997–1.153) $\times 10^{-3} \text{ mm}^2/\text{s}$	0.654
PDAC (n = 71)	1.376 (1.270–1.510) $\times 10^{-3} \text{ mm}^2/\text{s}$	1.380 (1.246–1.525) $\times 10^{-3} \text{ mm}^2/\text{s}$	0.778

Data are expressed as median (interquartile range)

ADC apparent diffusion coefficient, *AIP* autoimmune pancreatitis, *PDAC* pancreatic ductal adenocarcinoma

Table 4 Comparison of MRI findings between localized AIP and PDAC

MRI findings	Localized AIP (n = 40)	PDAC (n = 71)	P value
Hypointense capsule-like rim	32.5% (13/40)	0% (0/71)	<0.001
Speckled/dotted enhancement on the pancreatic phase	81.5% (22/27)	29.6% (8/27)	<0.001
Delayed homogeneous enhancement	81.5% (22/27)	22.2% (6/27)	<0.001
Duct penetrating sign	57.5% (23/40)	8.5% (6/71)	<0.001
MPD upstream dilatation ≤ 4 mm	77.5% (31/40)	29.6% (21/71)	<0.001

Data are percentages and numbers in parentheses refer to numbers of lesions

AIP autoimmune pancreatitis, PDAC pancreatic ductal adenocarcinoma, MPD main pancreatic duct

Table 5 Diagnostic performance of MRI findings for diagnosing localized AIP in 54 patients undergoing gadolinium-enhanced MRI

MRI findings	Sensitivity	Specificity	Accuracy	Odds ratio*
Hypointense capsule-like rim	37.0% (10/27)	100% (27/27)	68.5% (37/54)	∞
Speckled/dotted enhancement on the pancreatic phase	81.5% (22/27)	70.4% (19/27)	75.9% (41/54)	10.5 (2.9–37.4)
Delayed homogeneous enhancement	81.5% (22/27)	77.8% (21/27)	79.6% (43/54)	15.4 (4.1–58.2)
Duct penetrating sign	55.6% (15/27)	92.6% (25/27)	74.1% (40/54)	15.6 (3.1–79.6)
MPD upstream dilatation ≤ 4 mm	81.5% (22/27)	70.4% (19/27)	75.9% (41/54)	10.5 (2.9–37.4)
ADC value $\leq 1.188 \times 10^{-3}$ mm ² /s	92.6% (25/27)	88.9% (24/27)	90.7% (49/54)	100 (15.3–652.0)
Two or more MRI findings excluding ADC value	92.6% (25/27)	77.8% (21/27)	85.2% (46/54)	43.8 (8.0–240.0)
ADC value $\leq 1.188 \times 10^{-3}$ mm ² /s + one or more MRI findings	92.6% (25/27)	96.3% (26/27)	94.4% (51/54)	325 (27.7–3813.2)

Data are percentages and numbers in parentheses refer to numbers of lesions

*The ranges in parentheses refer to 95% confidence intervals. ∞ indicates that the odds ratio is infinity

AIP autoimmune pancreatitis, MPD main pancreatic duct, ADC apparent diffusion coefficient

that 6 (35.3%) of 17 patients with mass-forming AIP of the pancreatic head were misdiagnosed with PDAC and underwent surgical resection or bypass surgery. In their study, biopsy was performed in only six patients, but there have been reports of localized AIP surgically resected due to difficult differentiation even by EUS-FNA [32–34]. On imaging examination, MRI finding such as hypointense capsule-like rim, speckled/dotted enhancement on the pancreatic phase, delayed homogeneous enhancement, duct penetrating sign, and MPD upstream dilatation ≤ 4 mm have been reported to be useful in differentiating localized AIP from PDAC [14, 20–22, 26–29]. In this study, the finding of ADC value $\leq 1.188 \times 10^{-3}$ mm²/s showed better sensitivity, accuracy, and odds ratio than the MRI findings above, and a further improvement in diagnostic performance was obtained by adding the ADC value $\leq 1.188 \times 10^{-3}$ mm²/s to other MRI findings. DWI does not require a contrast agent, so it can be used in patients with reduced renal function or allergy to contrast agents. Furthermore, ADC values are quantitative data and considered to be more objective than other MRI findings.

DWI is an MRI technique based on the Brownian motion of water molecules in tissue. In tissues where cells proliferate densely, such as carcinomas, fibrosis, and edema, the

diffusion of water molecules is suppressed and a hyperintense signal is drawn on the DWI as an abnormal signal, while the ADC value is low. PDAC often shows lower ADC values than the normal pancreas [16, 35], which has been reported to be caused by increased cell density and fibrosis associated with tumor invasion (desmoplastic reaction) [35]. On the contrary, autoimmune pancreatitis has a characteristic pathological tissue called lymphoplasmacytic sclerosing pancreatitis, consisting of marked infiltration of lymphocyte and plasma cell and fibrosis, infiltration of numerous IgG4-positive plasma cells, storiform fibrosis, and obliterative phlebitis [36]. A marked increase in cell density due to lymphocyte or plasma cell infiltration in addition to fibrosis appears to be the main reason why AIP has lower ADC values than PDAC.

In this study, MRI was performed to assess the effects of steroids at a mean of 7.9 days after induction of steroids, and a significant increase in ADC values was shown. Diagnosis of localized AIP often requires evaluation of steroid responsiveness. Moreover, in this study, one-third of the patients required the assessment of steroid responsiveness to diagnose AIP. Moon et al. [37] evaluated the findings of CT and endoscopic retrograde cholangiopancreatography/MRCP after 2 weeks of steroid therapy in 22 suspected

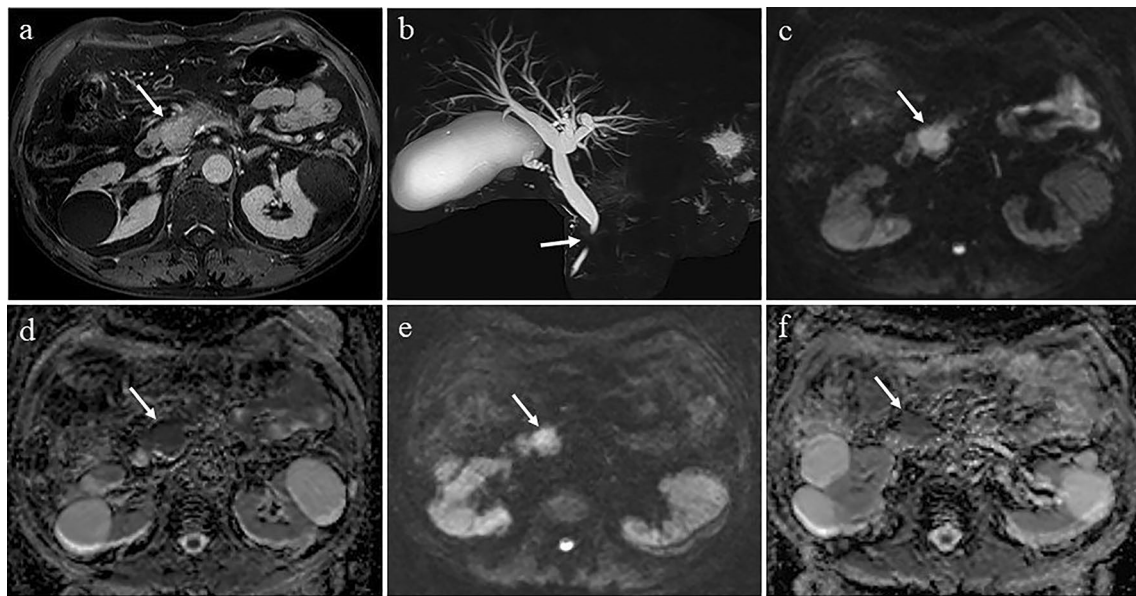


Fig. 5 A 70-year-old man with localized type 1 autoimmune pancreatitis. **a** Delayed-phase magnetic resonance image shows the pancreatic head mass relatively homogeneously enhanced (arrow). **b** MRCP image shows the stricture of the lower extrahepatic bile duct (arrow). **c** DWI at $b = 1000 \text{ s/mm}^2$ before steroid therapy. The mass in the pancreatic head shows hyperintense signal (arrow). **d** ADC map of the same lesion. The mass shows hypointense signal (arrow), and

the ADC value of the mass was $1.068 \times 10^{-3} \text{ mm}^2/\text{s}$. **e** DWI 7 days after induction of steroid therapy. The signal intensity of the mass had decreased (arrow). **f** ADC map of the same lesion. The ADC value of the mass (arrow) was $1.438 \times 10^{-3} \text{ mm}^2/\text{s}$. *MRCP* magnetic resonance cholangiopancreatography, *DWI* diffusion-weighted imaging, *ADC* apparent diffusion coefficient

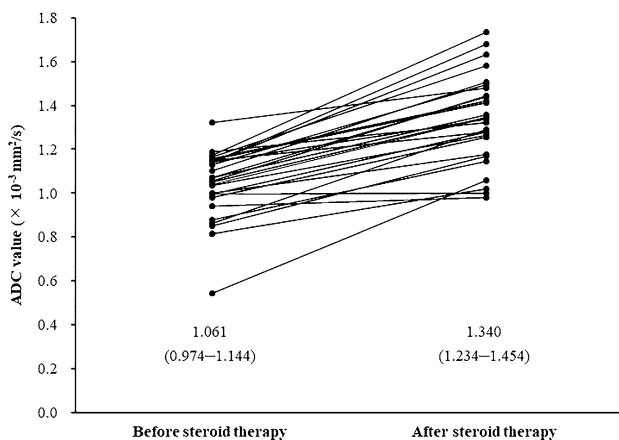


Fig. 6 Comparison of ADC values before and after induction of steroid therapy in localized autoimmune pancreatitis. *ADC* apparent diffusion coefficient

AIP patients. All 15 AIP patients showed improvement on the image, and 7 patients without improvement on the image were finally diagnosed with PDAC. In addition, Yukutake et al. [38] recommended evaluating pancreatic enlargement and pancreatic duct images on day 8 after steroid induction. No evidence showed that short-term administration of a moderate dose (0.6 mg/kg/day)

of steroids with immunosuppressive effect influences the surgical outcomes and long-term prognosis of PDAC, but steroid administration to PDAC should be kept as short as possible. Several studies have reported that the ADC values at AIP lesion site increased after steroid induction [19, 23, 24]. However, these reports have problems such as a very small sample size, a long period from steroid induction to re-evaluation of the ADC value, and no mention of the number of days from steroid induction to re-evaluation of the ADC value. The results of this study suggest that ADC values can be an objective and rapid method of assessing steroid responsiveness in localized AIP in 1–2 weeks.

In previous reports [19–23], the ADC values of AIP showed a certain range of $0.790 \times 10^{-3} \text{ mm}^2/\text{s}$ to $1.086 \times 10^{-3} \text{ mm}^2/\text{s}$. Possible reasons for this disparity include settings of DWI imaging parameters, activity of AIP, and the like. However, the setting condition of b value has the highest effect. Muhi et al. [20] reported an ADC value of $0.790 \times 10^{-3} \text{ mm}^2/\text{s}$ in mass-forming AIP, which was much lower than other reports. This difference is probable due to the following reason; unlike other studies that measured ADC with two b values of 0 and 500–1000 s/mm^2 , Muhi et al. used b values of 500 and 1000 s/mm^2 to reduce the effects of T2 shine-through and perfusion. Thus, it is necessary to evaluate the ADC value by understanding that it is

not an absolute value and is affected by the setting condition of the imaging parameters.

In this study, although ADC values were measured using two MRI scanners with different field strength at different times, no difference was found in ADC values between the scanners for both localized AIP and PDAC. Xiao et al. [39] reported that the ADC values of pancreas were affected by the field strength of scanner. On the other hand, Ogura et al. [40] reported that if the appropriate imaging parameters (repetition time, > 3000 ms; echo time, minimum; and high signal-to-noise ratio of high-b DWI) were used, the variability in ADC values for different MR scanners was fairly small. All imaging parameters used in this study met these conditions. When ADC values are used for diagnosing localized AIP, it is necessary to pay attention to the setting of the imaging parameters described above.

This study has several limitations. First, it was a retrospective study and some selection bias was inevitable. Second, although our study analyzed the largest number of patients among previous studies on ADC values of localized AIP, it was by no means large enough. Still, AIP is a relatively rare disease [30], and it is not easy to accumulate the number of patients. Third, the relationship between ADC values and histopathological findings has not been clarified. Although resected specimens can be evaluated for histopathological findings, surgical resection was performed in only four localized AIP patients. Further, while EUS-FNA was performed in most patients, it is difficult to evaluate the degree of inflammatory cell infiltration and fibrosis with such small specimens. Lastly, *b* values of 0 and 1000 s/mm² were used in the measurement of ADC values, and ADC values appear to have been measured slightly higher due to the perfusion effect. It is necessary to consider measuring ADC values by eliminating the effect of perfusion using methods such as the use of 200 s/mm² or more as a low *b* value and the intravoxel incoherent motion–DWI model [41].

In conclusion, ADC values were useful for the differential diagnosis of localized type 1 AIP and PDAC, and the early determination of the effect of steroid therapy. In localized type 1 AIP where diagnosis is difficult, the measurement of ADC values can be helpful in diagnosis.

Acknowledgements The authors would like to thank Takayuki Tamura, Department of Radiology, Hiroshima University Hospital for comments on the MRI techniques, and Editage (www.editage.jp) for English language editing.

Author contributions TS analyzed the data and wrote the manuscript. YI designed the study and contributed to the analysis and interpretation of the data, and assisted in the preparation of the manuscript. MS, TT, RK, KT, SN, TH, AF, TM, JI, YK, SS, YT, SM contributed to data collection. KC critically reviewed the manuscript. All authors read and approved the final version of the manuscript.

Funding Not applicable.

Data availability The datasets used and analyzed during the current study are available from the corresponding author on reasonable request.

Compliance with ethical standards

Conflict of interest The authors declare no relationships with any companies, whose products or services may be related to the subject matter of the article.

Ethical approval This study was conducted in accordance with the Declaration of Helsinki and was approved by the Ethical Committee for Epidemiology of our institution (Approval No. E-1949).

Consent to participate The written informed consent was waived by the Institutional Review Board because this was a retrospective study of clinical and image data.

References

- Shimosegawa T, Chari ST, Frulloni L, et al (2011) International consensus diagnostic criteria for autoimmune pancreatitis: guidelines of the international association of pancreatology. *Pancreas* 40:352–358. <https://doi.org/10.1097/MPA.0b013e3182142fd2>.
- Notohara K, Burgart LJ, Yadav D, Chari S, Smyrk TC (2003) Idiopathic chronic pancreatitis with periductal lymphoplasmacytic infiltration: clinicopathologic features of 35 cases. *Am J Surg Pathol* 27:1119–1127. <https://doi.org/10.1097/00000478-200308000-00009>.
- The Japan Pancreas Society, The Research Program on Intractable Diseases from the Ministry on Labor and Welfare of Japan (2018) Japanese Clinical Diagnostic Criteria for Autoimmune Pancreatitis, 2018 (Proposal) –Revision of Japanese Clinical Diagnostic Criteria for Autoimmune Pancreatitis, 2011- [in Japanese with English abstract]. *J Jpn Pancreas (Suizo)* 33:26–37.
- Irie H, Honda H, Baba S, et al (1998) Autoimmune pancreatitis: CT and MRI characteristics. *AJR Am J Roentgenol* 170:1323–1327. <https://doi.org/10.2214/ajr.170.5.9574610>.
- Chen G, Liu S, Zhao Y, Dai M, Zhang T (2013) Diagnostic accuracy of endoscopic ultrasound-guided fine-needle aspiration for pancreatic cancer: a meta-analysis. *Pancreatology* 13:298–304. <https://doi.org/10.1016/j.pan.2013.01.013>.
- Banafea O, Mghanga FP, Zhao J, Zhao R, Zhu L (2016) Endoscopic ultrasonography with fine-needle aspiration for histological diagnosis of solid pancreatic masses: a meta-analysis of diagnostic accuracy studies. *BMC Gastroenterol* 16:108. <https://doi.org/10.1186/s12876-016-0519-z>. Banafea O, Mghanga FP, Zhao J, Zhao R, Zhu L (2016) Endoscopic ultrasonography with fine-needle aspiration for histological diagnosis of solid pancreatic masses: a meta-analysis of diagnostic accuracy studies. *BMC Gastroenterol* 16:108. <https://doi.org/10.1186/s12876-016-0519-z>.
- Ishikawa T, Itoh A, Kawashima H, et al (2012) Endoscopic ultrasound-guided fine needle aspiration in the differentiation of type 1 and type 2 autoimmune pancreatitis. *World J Gastroenterol* 18:3883–3888. <https://doi.org/10.3748/wjg.v18.i29.3883>.
- Morishima T, Kawashima H, Ohno E, et al (2016) Prospective multicenter study on the usefulness of EUS-guided FNA biopsy for the diagnosis of autoimmune pancreatitis. *Gastrointest Endosc* 84:241–248. <https://doi.org/10.1016/j.gie.2016.01.016>.
- Kanno A, Masamune A, Fujishima F, et al (2016) Diagnosis of autoimmune pancreatitis by EUS-guided FNA using a 22-gauge

- needle: a prospective multicenter study. *Gastrointest Endosc* 84:797–804. <https://doi.org/10.1016/j.gie.2016.03.1511>.
10. Kurita A, Yasukawa S, Zen Y, et al (2020) Comparison of a 22-gauge Franseen-tip needle with a 20-gauge forward-bevel needle for the diagnosis of type I autoimmune pancreatitis: a prospective, randomized, controlled, multicenter study (COMPAS study). *Gastrointest Endosc* 91:373–381.e2. <https://doi.org/10.1016/j.gie.2019.10.012>.
 11. Okazaki K, Kawa S, Kamisawa T, et al (2014) Amendment of the Japanese Consensus Guidelines for Autoimmune Pancreatitis, 2013 I. Concept and diagnosis of autoimmune pancreatitis. *J Gastroenterol* 49:567–588. <https://doi.org/10.1007/s00535-014-0942-2>.
 12. Negrelli R, Manfredi R, Pedrinolla B, et al (2015) Pancreatic duct abnormalities in focal autoimmune pancreatitis: MR/MRCP imaging findings. *Eur Radiol* 25:359–367. <https://doi.org/10.1007/s00330-014-3371-y>.
 13. Yanagisawa S, Fujinaga Y, Watanabe T, et al (2017) Usefulness of three-dimensional magnetic resonance cholangiopancreatography with partial maximum intensity projection for diagnosing autoimmune pancreatitis. *Pancreatol* 17:567–571. <https://doi.org/10.1016/j.pan.2017.05.001>.
 14. Lee S, Kim JH, Kim SY, et al (2018) Comparison of diagnostic performance between CT and MRI in differentiating non-diffuse-type autoimmune pancreatitis from pancreatic ductal adenocarcinoma. *Eur Radiol* 28:5267–5274. <https://doi.org/10.1007/s00330-018-5565-1>.
 15. Koh DM, Collins DJ (2007) Diffusion-weighted MRI in the body: applications and challenges in oncology. *AJR Am J Roentgenol* 188:1622–1635. <https://doi.org/10.2214/AJR.06.1403>.
 16. Ichikawa T, Erturk SM, Motosugi U, et al (2007) High-b value diffusion-weighted MRI for detecting pancreatic adenocarcinoma: preliminary results. *AJR Am J Roentgenol* 188:409–414. <https://doi.org/10.2214/AJR.05.1918>.
 17. Park MJ, Kin YK, Choy SY, Rhim H, Lee WJ, Choi D (2014) Preoperative detection of small pancreatic carcinoma: value of adding diffusion-weighted imaging to conventional MR imaging for improving confidence level. *Radiology* 273:433–443. <https://doi.org/10.1148/radiol.14132563>.
 18. Qayyum A (2009) Diffusion-weighted imaging in the abdomen and pelvis: concepts and applications. *RadioGraphics* 29:1797–1810. <https://doi.org/10.1148/rg.296095521>.
 19. Kamisawa T, Takuma K, Anjiki H, et al (2010) Differentiation of autoimmune pancreatitis from pancreatic cancer by diffusion-weighted MRI. *Am J Gastroenterol* 105:1870–1875. <https://doi.org/10.1038/ajg.2010.87>.
 20. Muhi A, Ichikawa T, Motosugi U, et al (2012) Mass-forming autoimmune pancreatitis and pancreatic carcinoma: differential diagnosis on the basis of computed tomography and magnetic resonance cholangiopancreatography, and diffusion-weighted imaging findings. *J Magn Reson Imaging* 35:827–836. <https://doi.org/10.1002/jmri.22881>.
 21. Hur BY, Lee JM, Lee JE, et al (2012) Magnetic resonance imaging findings of the mass-forming type of autoimmune pancreatitis: comparison with pancreatic adenocarcinoma. *J Magn Reson Imaging* 36:188–197. <https://doi.org/10.1002/jmri.23609>.
 22. Choi SY, Kim SH, Kang TW, Song KD, Park HJ, Choi YH (2016) Differentiating mass-forming autoimmune pancreatitis from pancreatic ductal adenocarcinoma on the basis of contrast-enhanced MRI and DWI findings. *AJR Am J Roentgenol* 206:291–300. <https://doi.org/10.2214/AJR.15.14974>.
 23. Taniguchi T, Kobayashi H, Nishikawa K, et al (2009) Diffusion-weighted magnetic resonance imaging in autoimmune pancreatitis. *Jpn J Radiol* 27:138–142. <https://doi.org/10.1007/s11604-008-0311-2>.
 24. Klauß M, Maier-Hein K, Tjaden C, Hackert T, Grenacher L, Stieltjes B (2015) IVIM DW-MRI of autoimmune pancreatitis: therapy monitoring and differentiation from pancreatic cancer. *Eur Radiol* 26:2099–2106. <https://doi.org/10.1007/s00330-015-4041-4>.
 25. Kamisawa T, Okazaki K, Kawa S, et al (2014) Amendment of the Japanese Consensus Guidelines for Autoimmune Pancreatitis, 2013 III. Treatment and prognosis of autoimmune pancreatitis. *J Gastroenterol* 49:961–970. <https://doi.org/10.1007/s00535-014-0945-z>.
 26. Sun GF, Zuo CJ, Shao CW, Wang JH, Zhang J (2013) Focal autoimmune pancreatitis: radiological characteristics help to distinguish from pancreatic cancer. *World J Gastroenterol* 19:3634–3641. <https://doi.org/10.3748/wjg.v19.i23.3634>.
 27. Kim HJ, Kim YK, Jeong WK, Lee WJ, Choi D (2015) Pancreatic duct “iceberg sign” on MRI for distinguishing autoimmune pancreatitis from pancreatic ductal adenocarcinoma in the proximal pancreas. *Eur Radiol* 25:1551–1560. <https://doi.org/10.1007/s00330-014-3548-4>.
 28. Sugiyama Y, Fujinaga Y, Kadoya M, et al (2012) Characteristic magnetic resonance features of focal autoimmune pancreatitis useful for differentiation from pancreatic cancer. *Jpn J Radiol* 30:296–309. <https://doi.org/10.1007/s11604-011-0047-2>.
 29. Ichikawa T, Sou T, Araki T, et al (2001) Duct-penetrating sign at MRCP: usefulness for differentiating inflammatory pancreatic mass from pancreatic carcinomas. *Radiology* 221:107–116. <https://doi.org/10.1148/radiol.2211001157>.
 30. Kanno A, Masamune A, Okazaki K, et al (2015) Nationwide epidemiological survey of autoimmune pancreatitis in Japan in 2011. *Pancreas* 44:535–539. <https://doi.org/10.1097/MPA.00000000000000325>.
 31. Kamisawa T, Imai M, Yui Chen P, et al (2008) Strategy for differentiating autoimmune pancreatitis from pancreatic cancer. *Pancreas* 37:e62–67. <https://doi.org/10.1097/MPA.0b013e318175e3a0>.
 32. Matsumoto I, Shinzeki M, Toyama H, et al (2011) A focal mass-forming autoimmune pancreatitis mimicking pancreatic cancer with obstruction of the main pancreatic duct. *J Gastrointest Surg* 15:2296–2298. <https://doi.org/10.1007/s11605-011-1543-5>.
 33. Macinga P, Pulkertova A, Bajer L, et al (2017) Simultaneous occurrence of autoimmune pancreatitis and pancreatic cancer in patients resected for focal pancreatic mass. *World J Gastroenterol* 23:2185–2193. <https://doi.org/10.3748/wjg.v23.i12.2185>.
 34. Marinho R, Alves A, Pignatelli N, Nunes V (2019) Unclassified autoimmune pancreatitis mimicking pancreatic cancer. *J Surg Case Rep*. <https://doi.org/10.1093/jscr/rjy340>.
 35. Muraoka N, Uematsu H, Kimura H, et al (2008) Apparent diffusion coefficient in pancreatic cancer: characterization and histopathological correlations. *J Magn Reson Imaging* 27:1302–1308. <https://doi.org/10.1002/jmri.21340>.
 36. Kawaguchi K, Koike M, Tsuruta K, Okamoto A, Tabata I, Fujita N (1991) Lymphoplasmacytic sclerosing pancreatitis with cholangitis: a variant of primary sclerosing cholangitis extensively involving pancreas. *Hum Pathol* 22:387–395. [https://doi.org/10.1016/0046-8177\(91\)90087-6](https://doi.org/10.1016/0046-8177(91)90087-6).
 37. Moon SH, Kim MH, Park DH, et al (2008) Is a 2-week steroid trial after initial negative investigation for malignancy useful in differentiating autoimmune pancreatitis from pancreatic cancer? A prospective outcome study. *Gut* 57:1704–1712. <https://doi.org/10.1136/gut.2008.150979>.
 38. Yukutake M, Sasaki T, Serikawa M, et al (2014) Timing of radiological improvement after steroid therapy in patients with autoimmune pancreatitis. *Scand J Gastroenterol* 49:727–733. <https://doi.org/10.3109/00365521.2014.900822>.
 39. Xiao HY, Jia YG, Zheng HY, Yuan L (2014) Apparent diffusion coefficient reproducibility of the pancreas measured at different

- MR scanners using diffusion-weighted imaging. *J Magn Reson Imaging* 40:1375–1381. <https://doi.org/10.1002/jmri.24492>.
40. Ogura A, Tamura T, Ozaki M, et al (2015) Apparent diffusion coefficient value is not dependent on magnetic resonance systems and field strength under fixed imaging parameters in brain. *J Comput Assist Tomogr* 39:760–765. <https://doi.org/10.1097/RCT.000000000000266>.
41. Le Bihan D, Breton E, Lallemand D, Aubin ML, Vignaud J, Laval-Jeantet M (1988) Separation of diffusion and perfusion in intravoxel incoherent motion MR imaging. *Radiology* 168:497–505. <https://doi.org/10.1148/radiology.168.2.3393671>.

Publisher's Note Springer Nature remains neutral with regard to jurisdictional claims in published maps and institutional affiliations.